Thesis for the degree of Licentiate of Engineering

Dynamic contact stiffness and air-flow related source mechanisms in the tyre/road contact

Julia Winroth

Department of Civil and Environmental Engineering
Division of Applied Acoustics, Vibroacoustic Group
Chalmers University of Technology
Göteborg, Sweden, 2013

Dynamic contact stiffness and air-flow related source mechanisms in the tyre/road contact

Julia Winroth
© Julia Winroth, 2013

Dynamic contact stiffness and air-flow related source mechanisms in the tyre/road contact
Julia Winroth

Department of Civil and Environmental Engineering
Division of Applied Acoustics, Vibroacoustic Group
Chalmers University of Technology

Abstract

Two aspect of phenomena occurring in, and in the vicinity of the contact patch formed by a tyre rolling on a road are here investigated: 1. A detailed numerical time domain contact model is used to evaluate approximations of the tread response that are commonly embraced in tyre/road interaction models. 2. A statistical approach is applied in the search to quantify the contribution from air-flow related source mechanisms to the total tyre/road noise.

Effects of inertia and material damping when the tread is locally deformed are often neglected in many tyre/road interaction models. How the dynamic features of the tread affect contact forces and contact stiffness is here assess by simulating the detailed contact between an elastic layer and a rough road surface. The dynamic case, with an elastic layer impulse response extending in time, is compared with the case where the corresponding quasi static response is used. The results indicate that the significant effect of material damping may approximately be included as an increased stiffness in a quasi static tread model if not very detailed processes are to be predicted.

There are at least two main tyre/road noise generation mechanisms: tyre vibrations and air-flow related source mechanisms (commonly referred to as air-pumping). This study investigates the importance of air-flow related noise sources by employing the fact that their vehicle speed dependence differs from the noise produced directly by tyre vibrations. Results show that air-flow related sources are significant contributors to measured tyre/road noise. A comparison with results from calculated rolling noise indicates that tyre vibrations in/close to the contact may lead to noise with air-flow characteristics.

Keywords: Tyre/road noise, Tyre/road contact, Tread modelling, Air pumping, Air-flow related source mechanisms

List of publications

This thesis is based on the work contained in the following appended papers, referred to by roman numerals in the text:

Paper I
Importance of tread inertia and damping on the tyre/road contact stiffness
J. Winroth, P.B.U. Andersson and W. Kropp
Submitted to the *Journal of Sound and Vibration*

Paper II
The contribution of air-pumping to tyre/road noise.
J. Winroth, C. Hoever, W. Kropp and T. Beckenbauer
Proceedings of AIA-DAGA 2013, Merano, Italy. In press.

The following papers are not included in the thesis due to an overlap in content or a content going beyond the scope of this thesis:

Implementation of non-linear contact stiffness and adhesion in a numerical model for tyre/road contact
J. Winroth and P.B.U. Andersson
Proceedings of InterNoise 2010, June 13-16 2010, Lisbon, Portugal

Influence of tread inertia during deformation using a detailed numerical tyre/road contact model
J. Winroth and P.B.U. Andersson
Proceedings of 6th Forum Acusticum 2011, 27 June-1 July 2011, Aalborg, Denmark, p. 2431-2434

Evaluation of approximations used for the tread layer response and road surface roughness in numerical models of the tyre/road contact
J. Winroth and P.B.U. Andersson
18th International Congress on Sound and Vibration (ICSV) 2011, 10-14 July 2011, Rio de Janeiro, Brazil, p. 1666-1673

Acknowledgements

First I would like to thank my supervisors: Patrik Andersson and Wolfgang Kropp. The ocean of knowledge and spirit that you posses is both impressive and inspiring to me. I very much appreciate your effort and support.

To all at Applied Acoustics: PhD colleagues, students, teachers, staff, visitors and others. I am deeply grateful for the opportunity to be around all of you wise, devoted people. I want to be a sponge, soaking up as much as possible of your immense expertise, experience and know-how.

A special thanks to Gunilla Skog and Börje Wijk for all administrative help and technical support during the years.

To my family, relatives and friends: Thanks for being there, for your care and encouragement. I miss you tremendously during intense working times like these. It feels like I am lacking something essential, a vitamin, an anchor, presence? Whatever it is I can only get it by spending time with you.

Last but not least: Thank you Esmeralda! You make me smile and laugh *every* day.

Contents

Chapter 1
Introduction

1.1 Background

The contact between the tyre and the road surface is of major importance for the overall performance of the vehicle. It also has considerable consequences for the environment and the health of humans. The interaction of tyre and road essentially determines the tyre/road noise which is the most important contributor to road traffic noise in society, at least for higher vehicle speeds. The contact also affects the grip and hence both safety and speed capability. Rolling resistance is partly due to the deformation of the tyre tread during rolling, this causes energy dissipation and increases the fuel consumption of the vehicle. Wear of tyre and road is also caused by the tyre/road interaction, introducing both environmental and economical aspects.

Road traffic noise may increases the risk of cardiovascular diseases, causes sleep disturbances and annoyance, among other effects. Collections of well established research covering this growing problem can be found in publications from e.g. the World Health Organisation in Europe [1].

The three main contributors that are responsible for the total road traffic noise is roughly: Power train and exhaust noise being dominant at lower speeds. Tyre/road noise due to the contact between tyre and road surface with an importance that grows with speed. Aerodynamical noise sources that are indispensable at very high driving speeds. The importance of the the tyre/road noise part has increased during the last decays, partly due to the development of more quiet engines and exhaust systems. The new types of electric-drive vehicles with genuinely quiet engines also directs focus to the tyre/road noise. It can be attributed to two main generation mechanisms: tyre vibrations directly exciting the air around the tyre and a variety of air-flow related source mechanisms in and close to the contact patch.

The specific background of this thesis partly origins from an attempt to include adhesive forces in a similar small-scaled contact model as used in this work [2].

The question arose about the importance of including tread inertia and material losses and an investigation about these properties covers the first part of this work. The second part addresses a suspicion that a larger part of the tyre/road noise is produced by air-flow related sources than what has been previously known.

1.2   Aim

An intention with this work is to increase the understanding about small-scale tread behaviour. It is anticipated that this can assist in the development of prediction tools being able to capture detailed processes in the tyre/road contact like stick-snap/slip and air-flow in the contact patch.

To control and reduce tyre/road noise it is beneficial to understand the underlying noise sources and how their relative importance varies with respect to driving conditions, road surface and frequency. The contribution of air-flow related sources to the total tyre/road noise is investigated in this work with the aim of showing if and how important these type of sources are.

1.3   Outline

This thesis covers two areas which indeed have connections with each other but on the other hand are very different. To increase the readability and clarify the content, the work is divided in two parts.

Chapter 2 covers aspects of inertia and damping in numerical tyre/road contact modelling.

In *Chapter 3* a speed exponent approach is applied in the search to understand the air pumping phenomenon in tyre/road noise context.

Chapter 4 Summarises the conclusions of the included papers and opens up for future work to be done.

Paper I, contains an investigation of how including/excluding tread inertia and damping affects the contact between an elastic layer and a small patch of a rough road surface.

Paper II, presents the speed exponent approach to investigate different source mechanisms of tyre/road noise. The main aim is to get deeper understanding about the phenomenon commonly referred to as air-pumping.

1.4   Limitations

The scope of the included work is limited:

- The contact simulations are limited to an elastic layer with a rigid backing indenting a 2cmx2cm piece of rough road surface. Tread *block* dynamics is not covered in Paper I or in *Chapter 2*.

- The contact simulations in Paper I cover normal contact forces, tangential forces are not included.

- Noise due to tyre vibrations and air-flow related sources are considered in Paper II and *Chapter 3*. Turbulence as a source of tyre/road noise is not included in this work.

Chapter 2

Contact modelling including tread inertia and damping

This part is based on Paper I where the importance of tread inertia and material damping is investigated by simulating the detailed contact between an elastic layer and a rough road surface patch. Results show that the contact is stiffer when using a dynamic response of the elastic layer and it is mainly the damping in the elastic layer that causes this effect.

2.1 Tread and contact modelling

2.1.1 Tread basics

The tread is the outermost layer of the tyre structure making contact with the road. All traction, breaking and steering forces of a vehicle are applied through this contact. The tread should in addition provide resistance against wear. Normal tyre treads are patterned but in a research context it is common to use a slick tread to simplify studies of material properties and the influence of the road for example.

The tread material consists mainly of synthetic and/or natural rubber compounds giving a relatively soft, isotropic, and almost incompressible material with a Poisson's ratio close to 0.5. Oils, vulcanising chemicals, and fillers such as carbon black and silica are typical substances added to change the material characteristics. Vulcanisation is a process which increases the shear modulus by increasing the number of cross-links between polymer chains and polymer chains and fillers. Fillers are used to further change properties, e.g. increasing the modulus while reducing the loss factor. This gives a less pronounced frequency dependence of the modulus compared with uncrossed-linked rubbers that has clear terminal, plateau, transition and glassy zones. Generally, tread rubbers show stiffness that slowly increase with frequency and the behaviour is also dependent on the temperature. The tread studied in this work has viscous losses that grows with frequency.

2.1.2   Important concepts in tread modelling

Local deformation

For small excitation areas, the response of a structure will exhibit *local deformation* characteristics in addition to propagating waves. Local deformation is a spring-like behaviour of the surface layer, it exists only around the excitation point and does not transmit vibrational energy into the structure. Kropp [3] made one of the first investigations of the local deformation of tyres by measuring driving mobilities using different excitation areas. Local deformation of tyres was later also nicely shown by Andersson et al. [4] who found it both in mobility measurements and in results of the numerical two layer model by Larsson and Kropp [5]. One important conclusion of their work was that high frequency mobility measurements on tyres are strongly affected by the excitation area. The effect can even be seen in low frequencies for very small excitation areas. Figure 2.1 shows measured and modelled radial point mobility for different excitation areas. A conclusion was that high frequency tyre models must include the local deformation to be able to simulate the contact behaviour of the tyre at these frequencies.

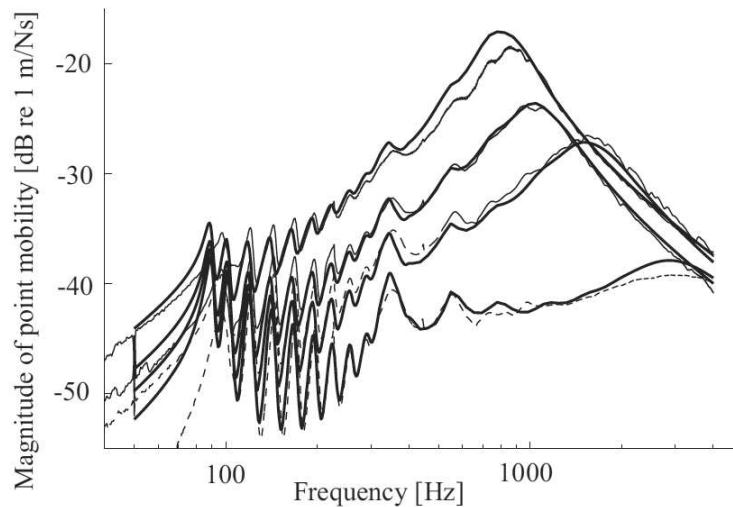Figure 2.1: Figure from [4], included here with permission from the author. Radial point mobility for a smooth tyre excited in the middle of the tread using four different excitation areas: calculated with excitation areas (all in millimetres) 2×2, 4×4, 6×6 and 15×15 (from top downwards in solid lines) and measured with excitation areas of radius of 2.3 mm, 4.5 mm, 6.9mm and 15 mm×15 mm (from top downwards in dashed lines).

Contact stiffness dependent/independent of load

Bodies making contact assert contact forces on each other. If at least one of them has a finite material stiffness some deformation/indentation will eventually occur. The contact stiffness is defined as the slope of the contact force-indentation curve. Assuming small indentation, a normal spring has a constant stiffness. An inherent property of the contact between bodies with rough surfaces is a non-linear contact formation. Contact will always initialise at a limited number of contact points. This gives a softer contact stiffness than a complete contact to the bulk material over the whole surface. As the rough surfaces approach each other more, the number of contact points and the contact stiffness grows. Saturation is near when the number of contact points does not increase as much and the contact stiffness approaches a constant value.

The spatial discretisation is crucial when modelling such process. What is seen as one contact point in a coarse resolution may consist of a dozen in a finer view, all entering the contact at different indentations. The tread is the part of the tyre that makes contact with the road roughness and a tread model with limited spatial resolution needs to consider the roughness on smaller length scales. This can be done in an approximative way by introducing linear contact springs. The stiffness of these is however difficult to assess and a common way is to tune them until the some output of the model approaches a measured quantity like apparent contact area or radiated noise. A more complete method is to use non-linear contact springs. Their stiffness functions can be approximated from a detailed scan of the road surface. More on non-linear contact springs is found in *Chapter 2.2.2*.

Required level of detail

The wide range of involved length scales complicates the modelling of tyre/road interaction. From the waviness of the road (meters) to the small-scale roughness of both tyre and road (micrometers and smaller). In addition there are a number of different processes affecting and being affected by the interaction like tyre vibrations, local deformation, different air-flow related noise sources, grip considerations including micro-scale adhesion and friction. It is not practical to build an efficient tyre/road interaction model that can predict all these processes on different length-scales using one fixed spatial resolution of the whole geometry, the requirements on e.g. spatial resolution and accuracy in material response are too different. A limited resolution and the use of constant contact springs has for example proven to work well for prediction of tyre vibrations and the estimation of rolling noise and rolling resistance [6]. Phenomenon on smaller length scales like air-flow in the contact patch, stick-slip/snap, adhesion, and friction may require more detailed models.

2.1.3   Different modelling approaches

Presented in the following are the most common ways to model the tread and the interaction between the tread and the road surface. Without claiming complete coverage of the respective fields, a few examples of research are also given.

The present tyre/road interaction model at Applied Acoustics, Chalmers, implements a tyre model in waveguide finite elements. To account for the road roughness on smaller length scales than the discretisation length, linear contact springs are used. The tread is modelled with solid elements and includes in this way inertia and material losses. More on this model is found in *Chapter 3.4.1* and in [7, 6, 8]. Finite element tyre models that includes the tread are limited to lower frequencies than the waveguide finite element models.

Linear springs has been used in several tyre/road interaction models to compute the contact forces that affects the tyre structure e.g. [9, 10]. Another example is Lopez et al. [11] where the rolling resistance of a tyre was investigated. The road texture induced rolling resistance was obtained by a 2D tyre/road interaction model where the tread was approximated by linear spring damper systems. The small-scale road roughness inside each element was accounted for by non-linear springs as suggested in [12]. Discrepancies between measurements and calculations was explained by the limitations of using a 2D interaction model.

An elastic half space is commonly used in rail/wheel interaction modelling and classical contact mechanics [13]. It is also implemented in tyre/road interaction by e.g. Wullens and Kropp [14]. In their rolling model the elastic half space was used in an iterative process together with tyre response Green's functions and 3D road roughness. The condition of the rolling contact is that the distance between the tyre rim and road surface is kept constant after the initial static loading phase where this distance is determined. More recently Dubois et al. [15] used the elastic half space to calculate tyre/road contact force spectra.

Models of a viscoelastic material has represented the tread in several tyre/road interaction models. Liu et al. [16] presented a model for predicting the contact forces between a tread block with viscoelastic properties and a rough road. Dubois et al. [17] compared a viscoelastic contact model to a purely elastic. They found a 20 % decrease of the contact area between elastic and viscoelastic cases but concluded that the static method could be sufficient if the stiffness of the material is correctly chosen.

2.2 The contact model

This chapter contains some features of the presently used contact model. A detailed description how the contact problem is set up and solved can be found in Paper I and in [12].

2.2.1 Simulations

The contact between an elastic layer and a rough road surface patch is simulated in this work. The main interest of the calculations is the resulting contact force and contact stiffness in the normal direction, and how they develop as a function of indentation (and for some cases time). Dynamic calculations with time evolution of the elastic layer impulse responses are compared with results obtained using a quasi static approximation.

Contact scenarios

Two contact scenarios are used, one where the layer is forced vertically into the road surface according to a predetermined indentation as a function of time. The second, preliminary case, describes the contact when the elastic layer is assigned an effective mass of 5 grams and released from different heights (0.1, 0.3 and 0.4 meter) above the road patch.

Three constant indentation accelerations are used in the first scenario to force the elastic layer into the road surface: 50 m/s^2, 250 m/s^2 and 500 m/s^2. Notice that accelerations in the order of 1000 m/s^2 are found for the tread on rolling tyres [18, 19].

The released mass scenario represents an extreme case with very low impedance behind the tread layer. A predetermined indentation function represents another extreme case with a very high impedance. The results of the two scenarios approach each other if the mass of the falling body is increased. The steady-state deformation of a tyre belt is to a large extent given by all the forces in the complete tyre/road contact, rather than just the local forces at such small contact patch under study here. Thus, a real tyre/road contact is expected to be closer to the high impedance case, but the extreme low impedance case is of interest for the fundamental understanding of the contact process.
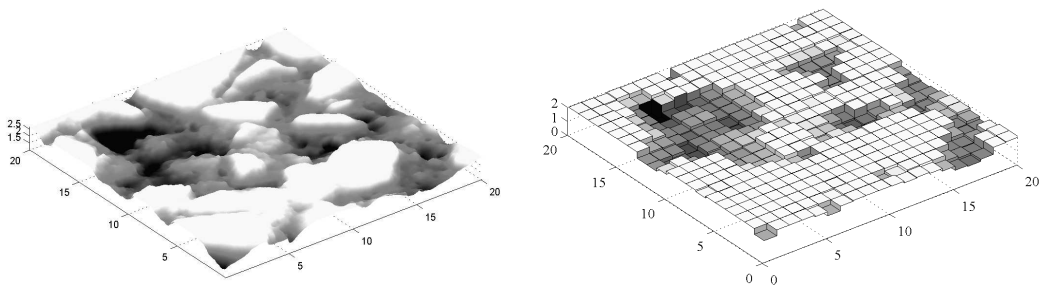
Time domain Green's functions of the elastic layer

The set of Green's functions representing the impulse response of the elastic layer is obtained by a modified version of the two-layered elastic plate model presented and validated in [20, 4]. The method yields frequency response functions which are transformed to the time domain by an inverse Fourier transform technique presented in [21]. The Green's functions in the present implementation are obtained using input data representing a 1.0 cm thick elastic layer with a perfectly rigid backing. A sampling frequency of 51.2 kHz is used and the resulting Green's functions are 256 samples long.

The quasi static approximation of the dynamic Green's function is the response that would be obtained if the layer had infinite wave speed and would react everywhere instantaneously. It consists only of a stiffness and neglects any effect of inertia or losses.

Road surface

The contact between the elastic layer and the road surface is made over an apparent area of 2×2 cm^2. The road surface data can be seen in Figure 2.2a. It originates from a high resolution scan of the wearing course of a road built according to the standard ISO-10844 [22]. The original resolution of the scan is 38 μm. The patch is then divided into 20×20 elements in the contact calculations, Figure 2.2b. This means that there will be 400 constant road element heights, 400 individual contact springs and 400 impulse response functions for the elastic layer.

(a) High resolution scan of the road surface.   (b)   Sampled version of the road surface containing 400 elements.

Figure 2.2: The 2×2 cm^2 road surface patch used in the simulations.

Resampling in the contact calculations

To avoid numerical instabilities that may occur in dynamic calculation for high indentations, a resampling technique is used. Basically the time resolution is increased by four by linear interpolation of the impulse response functions of the elastic layer. A comparison of calculations results using Green's functions originally having a four times higher sampling rate shows that this approach gives close to identical results.

Varying material parameters

Density and loss factor of the elastic layer are varied in the calculations as they are the two material parameters that cause the response of the layer to be a function of time.

The basic setting of the store and loss modulus are shown in Figure 3 in Paper I. The data is based on the typical behaviour found in measurements. Notice especially how the moduli increases with frequency. When varying the loss factor, the absolute value of the Young's modulus is kept constant to preserve the material stiffness.

Varying the density of the elastic layer within reason is not expected to give major effects on the contact force. The force required to accelerate a $2{\times}2{\times}1$ cm^3 free, rigid segment of the elastic layer to 500 m/s^2 is on the order of a few Newton. This is a small fraction of the forces present during normal tyre/road contact conditions. This expectation is confirmed by results in Paper I where a doubling of the elastic layer density gave more pronounced ripples in the stiffness function but the same saturated contact stiffness as in the reference case. The investigation is here extended to excessive changes of the elastic layer density: a tenfold increase and decrease of the default density of 1100 kg/m^3 is implemented in contact calculations.

2.2.2 Small-scale roughness contact springs

A numerical tyre/road interaction model must employ spatial discretisation of the contact. The question arises how to handle surface roughness on smaller length scales than the discretisation length, i.e. the roughness within the elements. The most simple approach is to neglect this information and basically "flatten" the surface of each element, resulting in a overestimated contact stiffness. The approach used in this work is to use non-linear contact springs, a method directly

adopted from [12]. An in-between method is to use linear contact springs, recently implemented by e.g. Hoever and Kropp [7].

The stiffness of the non-linear contact springs is evaluated from a high resolution scan of the road surface by studying the area of contact as a function of depth. Each spatial element will have a unique distribution of roughness resulting in an individual stiffness-indentation function for every element. The end points of the stiffness functions are however the same. Before the outermost point of a road element meets the elastic layer, the stiffness is zero. When fully indented, all small-scale points are in contact and the stiffness is infinite. A sketch of a road element and how its internal small scale roughness is approximated by a non-linear spring is seen in Figure 2.3. As a last comment it should perhaps be clarified that inertia and damping is not included in the contact spring formulation.
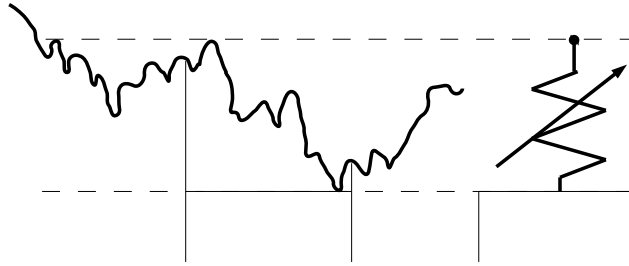

Figure 2.3: The softening effect of the surface roughness within one road element is approximated by a non-linear contact spring.

2.3 Results

2.3.1 Infinite indentation impedance

Results from Paper I are presented here for the simulation scenario of a predetermined indentation with constant acceleration. In addition to what is reproduced from Paper I, force-indentation relations are shown as well as simulations with extreme variation of elastic layer density. Contact forces are presented but similar results are obtained when studying the pressure at the interface between the elastic layer and the rigid backing.

The quasi static and the dynamic results show similar general behaviour with an initial non-linear phase which then approaches a linear state for larger indentations, Figure 2.4. The saturated contact stiffness is however substantially higher

when using a dynamic response and it increases with increasing indentation acceleration, Figure 2.4b. The stiffness function experiences a spasmodic increase for the fastest indentations whereas the quasi static has a smooth increase. In general, the number of elements in contact grows rapidly up to an indentation of around 0.05 mm and the contact stiffness follows the same trend. At an indentation of 0.15 mm, about 50% of the total number of elements are in contact.

(a) Contact force as function of indentation for different predetermined indentation accelerations and the quasi static case.

(b) Contact stiffness as function of indentation for different predetermined indentation accelerations and the quasi static case.
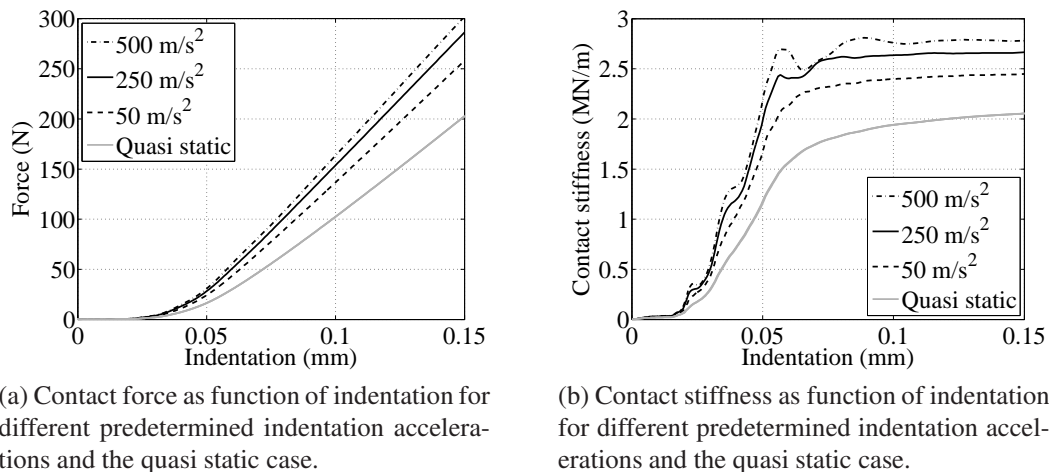
Figure 2.4: Results for different predetermined indentation accelerations and the quasi static case.

Results when varying the loss factor are shown in Figure 2.5 for the case of a predetermined indentation acceleration of 500 m/s^2. Increasing the loss factor of the elastic layer material gives a slightly stiffer dynamic contact and vice versa. The character of the stiffness curve is though similar to the reference case. The change in the saturated contact stiffness is small, around 3 % for a 50 % variation of the loss factor. The quasi static results are unaffected by changes in loss factor as the material stiffness is kept constant.

Increasing the density with a factor ten results in an extended initial non-linear contact phase giving very pronounced mass effects in the stiffness function with strong ripples, Figure 2.6. Lowering the density with a factor ten does not give corresponding differences. The saturated contact stiffness is not changed by density variations. This was also seen in the results for more moderate density changes presented in Paper I.
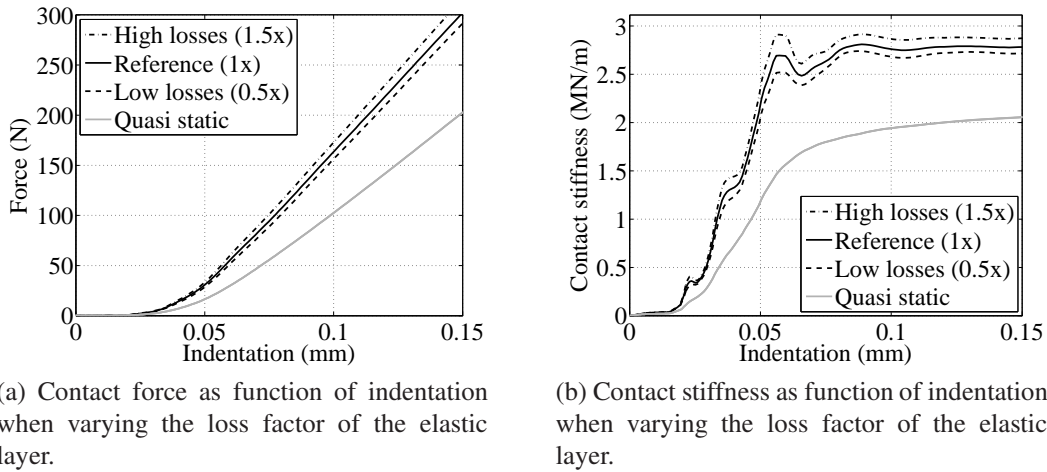
(a) Contact force as function of indentation when varying the loss factor of the elastic layer.

(b) Contact stiffness as function of indentation when varying the loss factor of the elastic layer.

Figure 2.5: Results when varying the loss factor of the elastic layer. A predetermined indentation acceleration of 500 m/s^2 is used.

(a) Contact force as function of indentation when varying the density of the elastic layer.

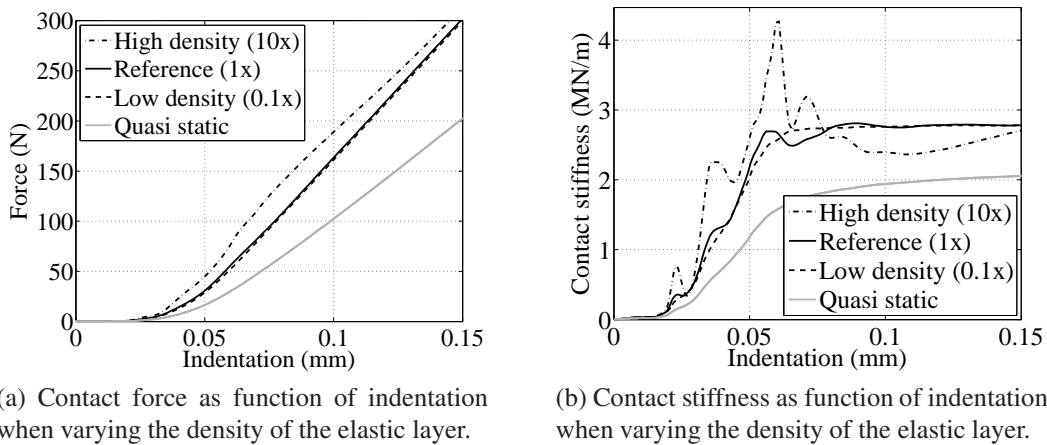(b) Contact stiffness as function of indentation when varying the density of the elastic layer.

Figure 2.6: Results when varying the density of the elastic layer. A predetermined indentation acceleration of 500 m/s^2 is used.

2.3.2   Indentation with a mass impedance

The contact case of a 5 gram mass released from different heights above the elastic layer is shown in Figure 2.7. There are major differences between dynamic and quasi static simulations. The most prominent is that the hysteresis becomes apparent in the dynamic contact force giving higher contact stiffness when entering the contact than when receding, Figure 2.7a. The quasi static results give similar force-indentation curve for entering and exiting as well as for different drop heights. The time development of the contact force, Figure 2.7b, reveals that the contact force develops faster in the dynamic case compared to the quasi static.

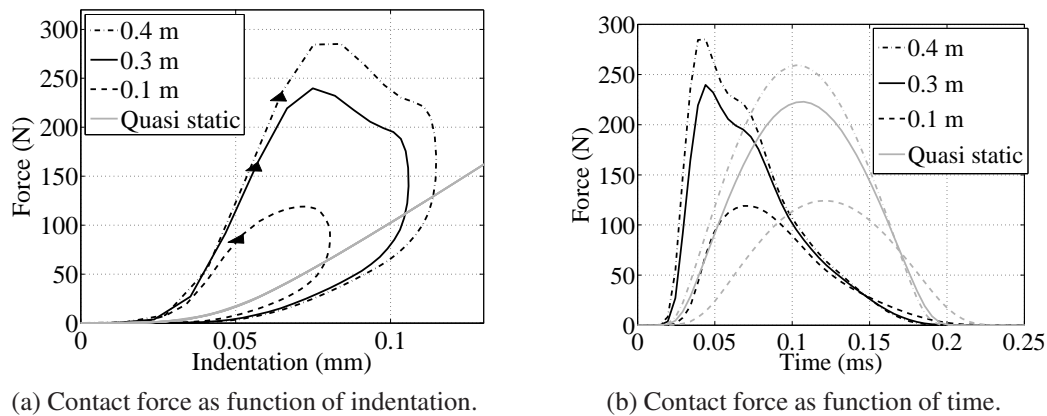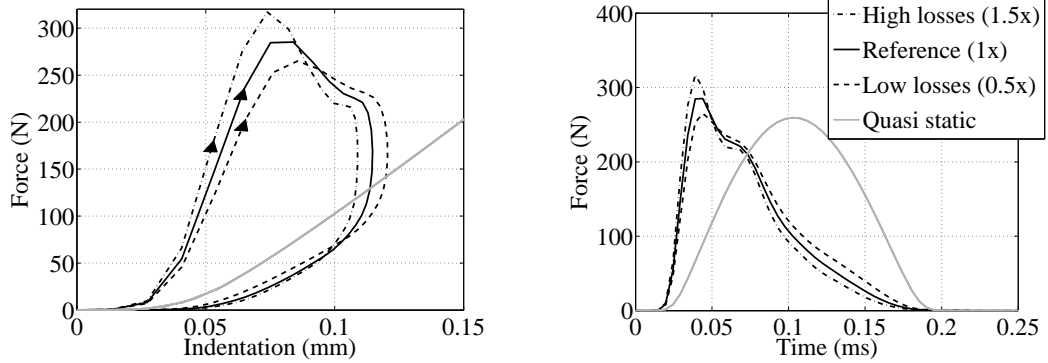(a) Contact force as function of indentation.   (b) Contact force as function of time.

Figure 2.7: Dynamic and quasi static simulations of the contact between the elastic layer and a 5 gram mass falling from three different heights.

Material parameters of the elastic layer were also varied in the contact scenario of a 5 gram mass released from 0.4 meter. Increasing the loss factor of the elastic layer material gives a slightly stiffer dynamic contact and vice versa, Figure 2.8. As in the infinite contact impedance scenario (Figure 2.5), variations of loss factor does not change the character of the contact.
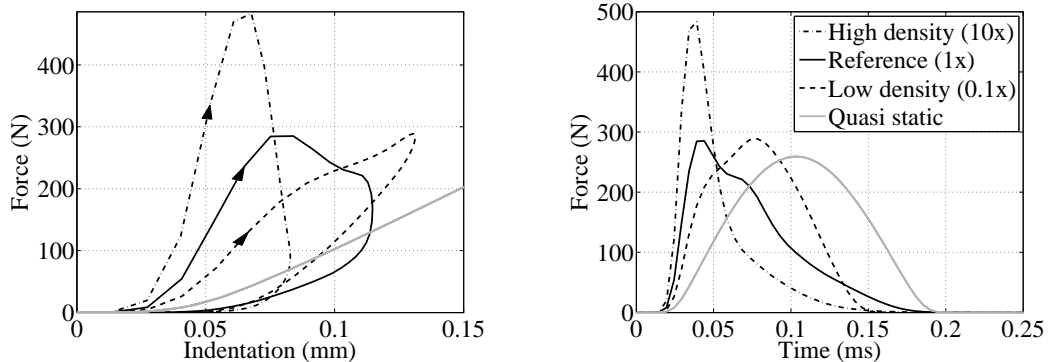
The variations in the results when varying density are more pronounced in the released mass scenario, Figure 2.9a, than compared with the case of an infinite contact impedance (Figure 2.6a). Increasing the density results in a much stiffer contact with a high peak contact force compared with the reference case. Decreasing density correspondingly results in a much lower contact stiffness and a deeper peak indentation instead. The development of the contact force with time is shown in Figure 2.9b. The peak force is obtained very fast for the heaviest material, for which it also decays rapidly. In the reference case the peak force is obtained roughly as fast but the decay is much slower. The low density case is slow, it approaches the quasi static simulation.

(a) Contact force as function of indentation when varying the loss factor of the elastic layer.

(b) Contact force as function of time when varying the loss factor of the elastic layer.

Figure 2.8: Results when varying the loss factor of the elastic layer. Simulation of a 5 gram mass falling from 0.4 meter above the layer.

(a) Contact force as function of indentation when varying the density of the elastic layer.

(b) Contact force as function of time when varying the density of the elastic layer.

Figure 2.9: Results when varying the density of the elastic layer. Simulation of a 5 gram mass falling from 0.4 meter above the layer.

2.3.3 Discussion

It should be emphasised that the contact case of a falling mass is preliminary at the present stage. The difference between the two contact scenarios is however interesting. Even if neither of them is an exact simulation of a real tyre/road contact event, they constitute two extremes. One where the contact is forced with an infinite impedance and one where there is only a small mass impedance and a initial velocity acting against the contact forces.

The most important factor separating dynamic from quasi static simulations seems to be how fast the indentation occurs. This is perhaps most clear when studying the results for the infinite impedance scenario. The character of the dynamic results is more or less similar to the quasi static, just stiffer. This implies that it might be possible to use a quasi static approach and account for the dynamic properties by a stiffening factor. This factor could also be a function of speed.

Material damping and mass are the two modelling parameters that cause differences between dynamic and quasi static simulations. Varying these parameters within reason has however shown to have a limited effect on the difference.

Material damping has a significant effect on the saturated contact stiffness in the case of an infinite contact impedance. But the character of the contact is unaffected by changes in loss factor, also seen in the contact scenario with a falling mass. This indicates that the effect of material losses could approximately be included as an increased stiffness in a quasi static tread model. If detailed behaviour at the tyre/road interface is to be simulated, e.g. for friction calculations, it may still require losses to be included more accurately.

The major effect of material density is ripples on the stiffness function during the initial indentation. These ripples are small for reasonable density values but grow large for very heavy material. Variations of the density, whether reasonable or not, do however not give any significant effect on the contact stiffness after saturation. The results for the falling mass contact scenario partly point in another direction. Here (drastic) changes of density give different character of the contact force as a function of indentation. This may be connected to the difference in time evolution of the contact force but further investigations are needed to explain these results. As a preliminary conclusion it is still believed that inertial effects only are of importance for very detailed modelling of interfacial behaviour.

2.4   Conclusions and future work

This work has investigated the importance of tread inertia and damping for detailed tyre/road contact modelling. Results show that the dynamic contact stiffness depends on how the indentation grows with time, the faster the indentation the stiffer the contact. The quasi static simulations, neglecting inertia and losses, give a significantly softer contact than the dynamic case. Material damping was varied and it gives significant effects on the contact stiffness, higher loss factor gives a stiffer contact and vice versa. An extreme increase of density results in pronounced mass effects in the initial contact stiffness function. However, density does not affect the saturated contact stiffness.

The most simple tread models assume a purely elastic response. The results of this study imply that it is not sufficient to merely measure a quasi static stiffness of a tread material and use this directly in a tyre/road interaction model. Some kind of stiffening factor is necessary to account for the dynamic properties of the tread material. If higher accuracy in the modelling is needed the next step is to include material damping, e.g. by implementing a viscoelastic model for the tread material. Effects of tread mass could be of importance when studying details in the contact or when testing novel concepts including extremely soft and/or heavy tread materials.

In this work the loss factor grows with frequency, a slight extension could be to simulate a material which has reversed frequency dependence of the loss factor. It would also be interesting to evaluate a constant contact stiffness that grows with rolling speed in a complete tyre/road interaction model. This could for example be done in the present tyre/road interaction model at Applied Acoustics, Chalmers. Here contact springs with constant stiffness are presently implemented and their stiffness value have been shown to influence the simulated tyre/road noise [6].

Chapter 3

The speed exponent approach to air-pumping

Based on Paper II, an approach is developed which makes it possible to distinguish the contribution from air-flow related source mechanisms in a set of tyre/road noise data. Required input is rolling noise for a number of driving speeds. The results show that a surprising amount of the tyre/road noise can be attributed to air-flow related sources.

3.1   Air-flow related source mechanisms

3.1.1   Introduction

A common way to approach tyre/road noise (also adopted here) is to assume that it origins from two main generation mechanisms; Tyre vibrations radiating directly into the air and what is commonly referred to as "air-pumping" concentrated to the contact zone.

In the present work the term "air-pumping" is slightly misleading as it may be interpreted as referring to an idea, theory, or model of a specific noise source. The goal is instead to investigate the importance of a *collection* of possible noise sources. The key issue is that the sound pressure level created by this collection is assumed to have a speed exponent around 4. This means that the acoustic pressure they create, p^2, will be proportional to the vehicle speed to the power of four: $p^2 \sim U^4$, where U is speed. In turn, this implies that the collection consists of monopole-like sources as these are characterised by acceleration of a volume flow of air (or fluctuations of the volume flow rate). Hence, the expression *air-flow related source mechanisms* will mainly be used in the following.

The search to understand tyre/road noise from air-flow related source mechanisms spans over decades and includes an impressive complexity. There is nevertheless an unsatisfying lack of a bridge between theories of specific mechanisms and actual tyre/road noise. Missing is a complete model that simulates rolling noise and includes both noise due to tyre vibrations and noise due to the most important air-flow related source mechanism(s). On the way towards this goal it is useful to understand for which cases tyre vibrations are the dominant mechanisms and for which cases air-flow related sources are more important.

Traditionally tyre vibrations are considered as the main generation mechanism at low-mid frequencies while air-flow related sources dominate the high frequency range above 1000 Hz. There are however indications that air-flow related source mechanisms may be of importance even for low frequencies and vice versa. This motivates the approach suggested in *Chapter 3.2* where the influence of each of these two main noise sources is extracted from tyre/road noise data.

3.1.2   Literature

Presented in the following is an overview of some of the work that has been done in the search to model and understand air-flow related source mechanisms in the tyre/road interaction. In general, theories on specific excitation mechanisms are presented and discussed. It is difficult to find complete studies that connect theoretical models to actual tyre/road noise. A literature study also covering resonance phenomena in tyre/road contact is found in [23].

Hayden 1971 [24]
During rolling it is likely that there will be sudden outflow/inflow of air from cavities in the tread and in the road surface when the tyre enters/leaves the contact. These types of changes in the volume flow characterise an acoustic omnidirectional monopole source. Simplified cases were modelled in this paper; a tyre with a tread pattern consisting of grooves rolling on a smooth surface and the case of a slick tyre rolling on a road with cavities. By adding the contributions from each monopole source that is excited when the tread enters and leaves the contact, a fairly simple equation for the generated sound pressure level was presented. Hayden emphasised that both his model and measured total a-weighted tyre/road noise levels have a speed dependency approaching U^4. He also stressed that his model is simple and that tyre vibrations may be of importance for low speeds.

Ronnerberger 1989 [25]

Where Hayden's theory dealt with noise due to grooves in either the road or the tread, Ronneberger developed a theory for how sound can be generated and predicted for a slick tyre rolling on roughness peak(s). The approach is limited to the leading edge. The most simple case studied is an elastic half space pressed onto a roughness peak. A sharp roughness peak will displace a relatively large volume of tread material compared with the volume of the peak itself. Air will rush to this newly "freed" volume to equalise the pressure and this can work as an acoustic monopole source. Although there is no comment on it, it seems like Ronneberger's theory works in the opposite way to Hayden's where air instead is squeezed out in the leading edge. The theory is then extended to a slick treaded tyre rolling on real road surfaces where a few modelling parameters are to be estimated first. Measurements and predictions of radiated sound power spectrum show good agreement for high frequencies for all but very fast speeds.

Hamet et. al 1990 [26]

Openings in form of cylindrical cavities in an otherwise smooth road surface generate strong noise when they are run over by a slick tyre. This study investigated the generation of fluctuating pressure and how it depends on the geometry of the cavity and the vehicle speed with measurements and theory. It was shown that noise mainly radiated at the trailing edge when the cavity that had been under pressure during the contact was opened. A pressure pulse is first generated followed by a decay where the modes of the cavity with less damping survives longer. The maximum pressure inside the cavity was shown to depend on speed but there was no investigation on the speed dependency of the radiated sound pressure.

More recent work

Gagen [19] complicated the picture around sound generated by squeezed cavities in tyre/road contact. Walls of a groove may be subject to very high acceleration and velocities as the tread enters and deforms in the tyre/road contact. It is argued that the deformation of the tread happens faster then the air inside the groove can evacuate. This could give density fluctuations large enough to arrive outside the linear theory of acoustics including the simple acoustic monopole source. Gagen employs the *s*queezed wave equation for the behaviour of the air in the groove and argues that the small-amplitude, linear acoustic theory is incorrect for tread groove squeezing during tyre/road contact. What the difference in far field sound pressure would be when employing his theory instead of e.g. Hayden's is however not investigated. This was instead later studied by Kim et. al [27] who adopted the idea of Gagen that there is an important non-linearity to the "squeezed cavity" air-pumping noise source. They used a hybrid technique including computational fluid dynamics (CFD) calculations and a Kirchhoff integral method for the generated

far-field sound. It was concluded that using the non-linear type of source, very high frequency noise (2-8 kHz) increases as well as the directivity of the noise (in direction of travel and tyre axis). CFD is also used in the work by Conte and Jean [28] where the measurements of Hamet et. al [26] where simulated in 2D.

3.2   The speed exponent approach

The speed exponent of tyre/road noise has been discussed in the literature (e.g. [29]) but often surprisingly brief, only considering the total A-weighted sounds pressure level. The starting point of the present approach is that different acoustic sources have different speed dependencies. This difference in speed exponent can be used to identify the contribution of each mechanism in data sets of tyre/road noise.

Sound generation due to tyre vibrations is expected to be proportional to U^2 where U is the driving speed. The noise generation due to a time varying volume flow of air is expected to be proportional to U^4. The acoustic tyre/road noise pressure as a function of frequency f and driving speed, $p^2(f, U)$ is assumed to consist of these parts. Each part is described by a source coefficient A multiplied with the driving speed U raised to the power of the corresponding speed exponent. The total acoustic pressure is the sum of these (presumed) uncorrelated contributions:

$$p^2(f, U) = A_2(f, U) \cdot U^2 + A_4(f, U) \cdot U^4 \qquad (3.1)$$

If the underlying excitation can be assumed to depend only slightly on speed (i.e. the roughness spectrum is rather flat and only slick tyres are considered) the equation can be simplified to:

$$p^2(f, U) = A_2(f) \cdot U^2 + A_4(f) \cdot U^4 \qquad (3.2)$$

The contribution from the two tyre/road noise sources for a specific tyre/road combination is determined by applying this speed exponent approach to a set of noise spectra covering (a large) number of driving speeds. For each frequency, the strength of each source is found by a least square fit method determining the unknown amplitudes A_2 and A_4. Figure 3.3a shows a result for the 160 Hz third octave band where air-flow related mechanisms and tyre vibrations together explain the measurement results. It is clear form the figure that both mechanisms are needed to explain the measured sound pressure level in this frequency band. Other frequency bands are only explained by air-flow related source mechanisms, e.g. the 400 Hz band in Figure 3.3b.

3.3 Measurements

3.3.1 About the measurements

The measurement data that is analysed in this work origins from the Sperenberg project that was conducted at a former air-field in Sperenberg close to Berlin in Germany. It was a major measurement project where 3200 controlled pass-by (CPB) levels spectra were recorded. 16 different car tyres were tested on 38 dense and rigid road pavements with several nominal driving speeds in the range from 50 km/h to 120 km/h. More on the Sperenberg project can be found in [30].

The speed exponent approach is here applied on 1/3 octave band spectra produced at different vehicle speeds. The time signal used is a 125 ms piece of the CPB noise taken when the overall sound pressure level peaked. This introduces an uncertainty as it is not defined where the wheel actually is positioned when the time signal is recorded. Further measurements conducted at the Sperenberg as well as other test cites may provide more complete measurement data for future analysis.

In all cases but one a slick tyre has been used on three road surfaces that can seen in Figure 3.1: mastic asphalt (Figure 3.1a), single layer open porous asphalt (Figure 3.1b), and a sand paper road surface (Figure 3.1c). In Paper II there is also a result for a sealed stone mastic asphalt.
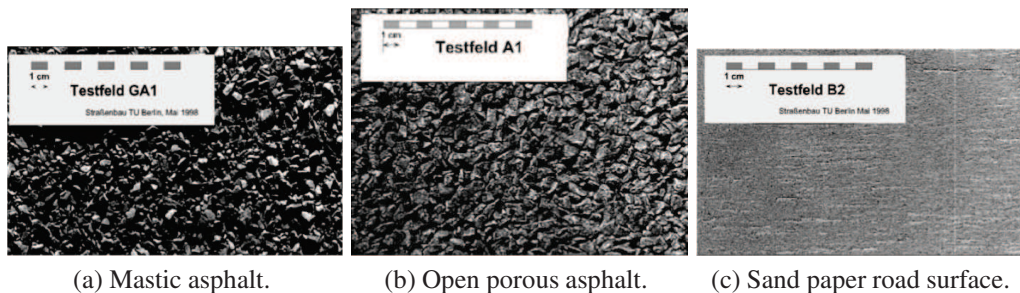

(a) Mastic asphalt.   (b) Open porous asphalt.   (c) Sand paper road surface.

Figure 3.1: The three road surfaces that are used in this work.

3.3.2   Results

The CPB measurement data set for a slick tyre on a mastic asphalt surface is seen in
Figure 3.2a. The spectrum looks like expected with a peak level around the 1000 Hz
band. Different speed dependencies of different frequency bands can already be
noticed in the data set. This is more clear when studying the contribution of air-
flow related sources in percentage of the total level, Figure 3.2b. It shows that for
low frequencies and low speeds tyre vibrations are the dominating noise source.
But for high frequencies, around the 800 Hz band and up, air-flow related sources
are dominating even for low speeds. Notice also how the 400 Hz band is completely
controlled by air-flow related sources. Some contribution from tyre vibrations can
be seen in the 2500 Hz band for low speeds, although this is quite weak.

(a) CPB level as a function of speed and
frequency.

(b) Contribution of air-flow related sources to the
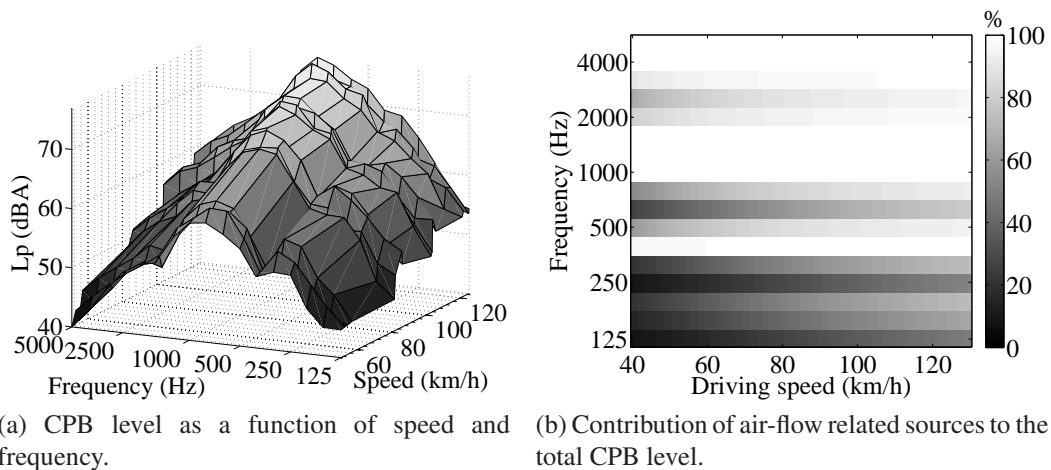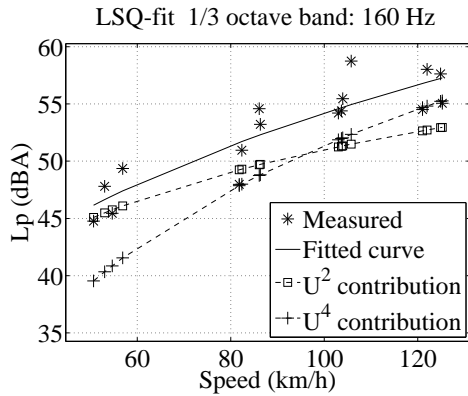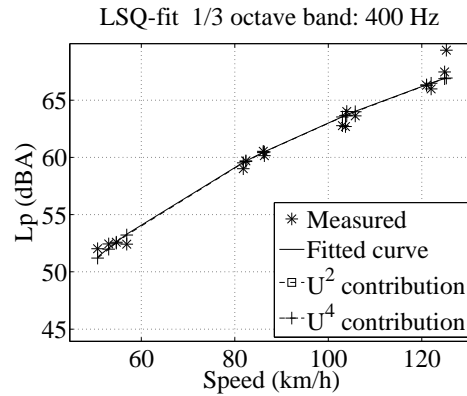total CPB level.

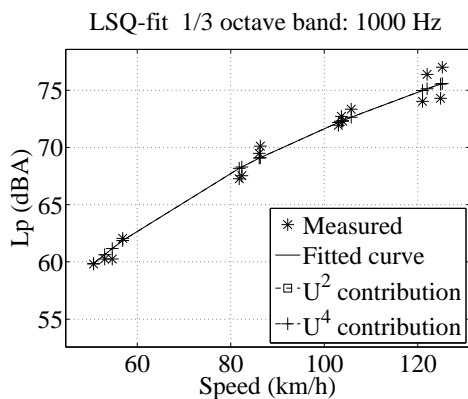Figure 3.2: Results for a slick tyre on mastic asphalt road surface.

Figure 3.3 shows examples of results for single frequency bands with the mea-
surement points and the fitted curve consisting of the contribution from tyre vibra-
tions (U^2) and air-flow related source mechanisms (U^4). The spread of the data is
generally larger for the lowest frequency bands, Figure 3.3a shows the result for
the 160 Hz band. In contrast, the 400 Hz band has very close measurement points,
Figure 3.3b. An idea could be that there is one dominating air-flow related source
mechanism in this band, resulting in this very stable appearance. For the lower
frequencies there might be a more complicated connection between different noise
sources giving higher uncertainties and a larger spread. Figure 3.3c and Figure 3.3d
show the results for the 1000 and 2500 Hz bands. The spread of the measurement
data is small and the fitted curve matches the points well. The weak tyre vibration
contribution at high frequency seen in Figure 3.2b is indeed slight, at the most
around 5 dB below the contribution from air-flow related sources.

(a) 160 Hz, relatively large spread in the low frequency data.

(b) 400 Hz, surprisingly only contribution from air-flow related sources.

(c) 1000 Hz, small spread in high frequency measurement data.

(d) 2500 Hz, weak tyre vibration contribution can be seen.

Figure 3.3: Single third octave band results, measurement points and the fitted curve consisting of the contribution from tyre vibrations and air-flow related source mechanisms for a slick tyre on mastic asphalt road surface.

Figure 3.4a shows the measurement data set for a slick tyre on a single layer open porous asphalt surface. The porosity of the road leads to absorption which can be seen as clear dips in the CPB level spectrum. The contribution of air-flow related sources relative to the total level is seen in Figure 3.4b. As for the mastic asphalt road surface, the very high frequencies are completely dominated by air-flow related sources. This is surprisingly also the case for the low frequency bands. It is only around 500-800 Hz where tyre vibrations is the main tyre/road noise generation mechanism.

(a) CPB level as a function of speed and frequency.

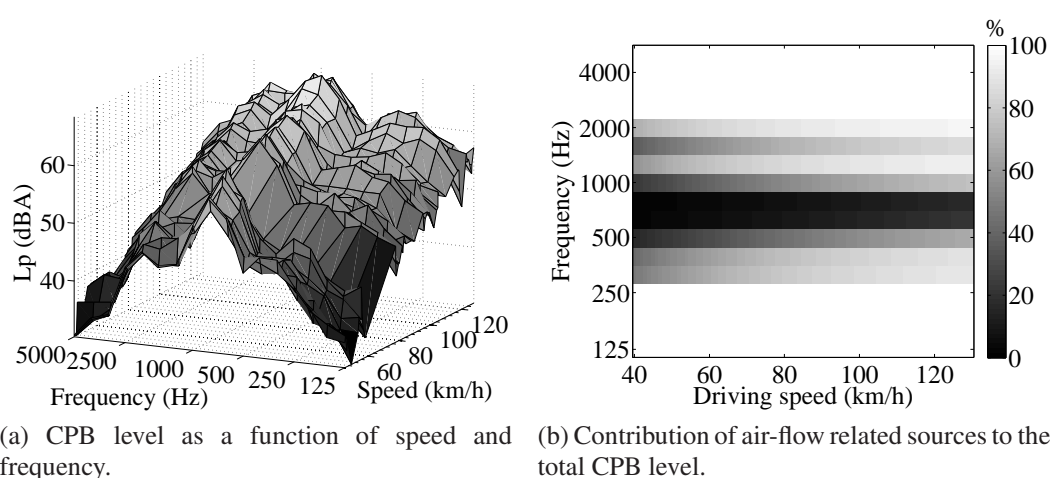(b) Contribution of air-flow related sources to the total CPB level.

Figure 3.4: Results for a slick tyre on a single layer open porous asphalt road surface.

Single frequency band results for a slick tyre on single layer open porous asphalt can be seen in Figure 3.5. The spread of the low frequency measurement data points, Figure 3.5a, is large also in this case (as with the previous mastic asphalt case). But the dominance of air-flow related sources in the low frequencies can not be questioned, on the contrary it is clear that there is indeed a very strong speed dependency. The 400 Hz band, Figure 3.5b, is also dominated by air-flow related sources except for low speeds where the vibrations are equally important. They grow more important for higher frequencies, the 800 Hz result is shown in Figure 3.5c, but the spread in the data is relatively large. The spread is smaller for very high frequencies, the 2000 Hz band result is shown in Figure 3.5d. The dominance of air-flow related source mechanisms are also clear here.

(a) 160 Hz, very strong speed dependence.

(b) 400 Hz, dominated by air-flow related sources.

(c) 800 Hz, representing a region dominated by tyre vibrations.

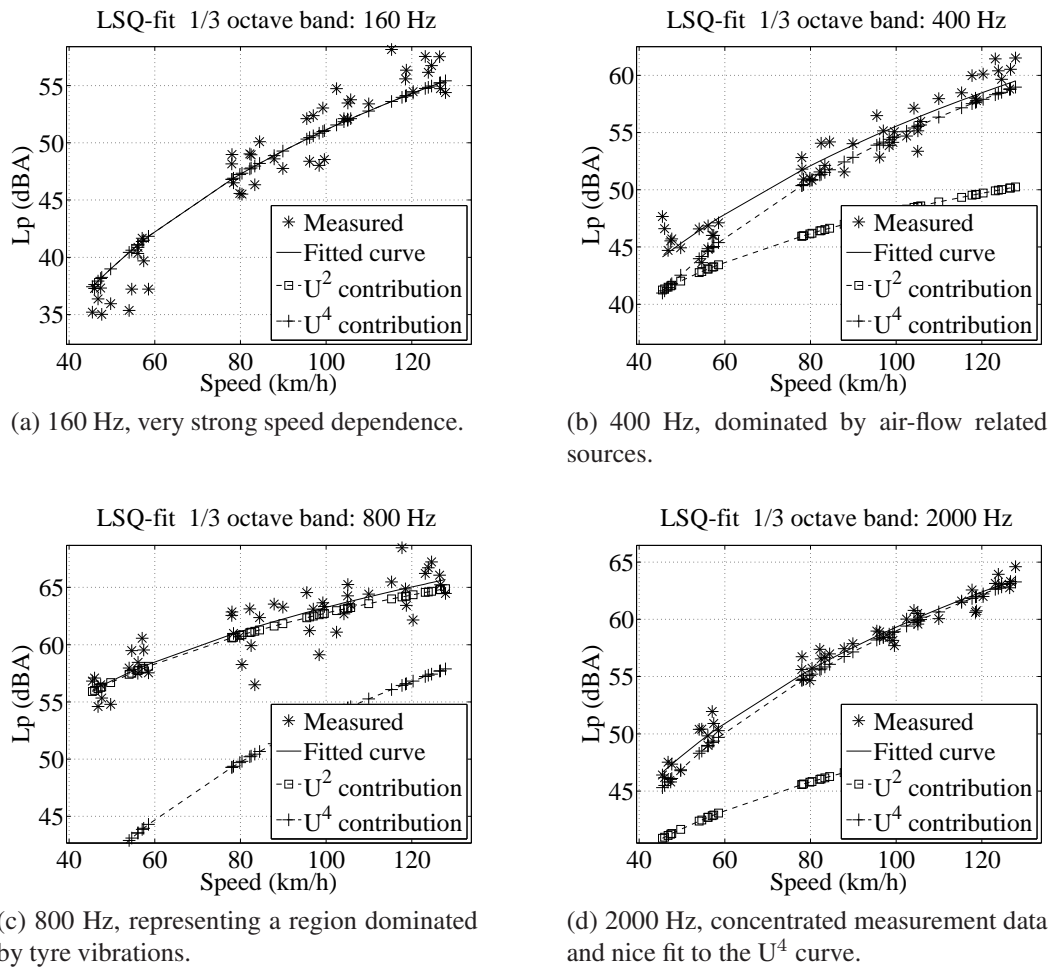(d) 2000 Hz, concentrated measurement data and nice fit to the U^4 curve.

Figure 3.5: Single third octave band results, measurement points and the fitted curve consisting of the contribution from tyre vibrations and air-flow related source mechanisms for a slick tyre on a single layer asphalt road.

The CPB measurement data set for a slick tyre on a sand paper type of road surface is seen in Figure 3.6a. The spectrum is more flat than for the previous shown roads but there is still a peak around the 1000 Hz band. Figure 3.6b reveals that the CPB levels are solely caused by air-flow related sources. It could be that the excitation of tyre vibrations is very weak due to the smoothness of the road. It could also be that the efficiency of some air-flow related source mechanisms increases dramatically with road smoothness.

(a) CPB level as a function of speed and frequency.

(b) Contribution of air-flow related sources to the total CPB level.
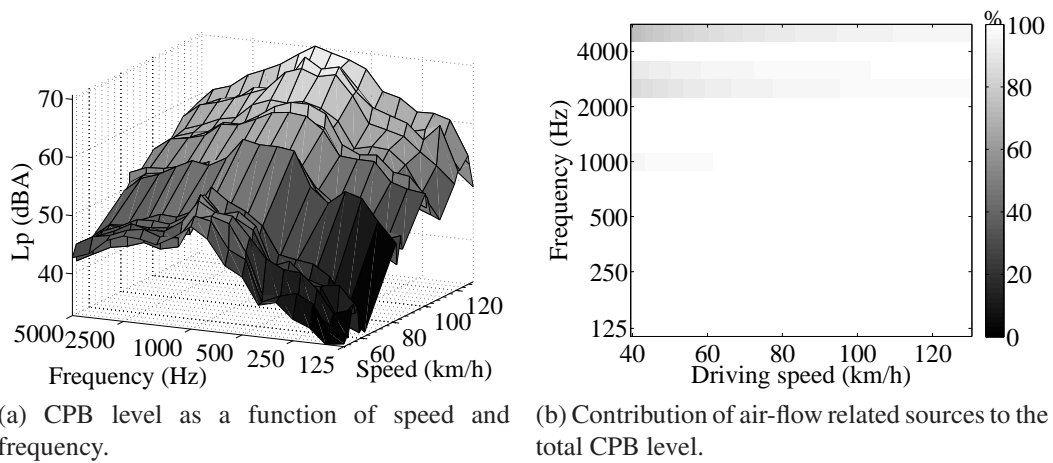
Figure 3.6: Results for a slick tyre on a sand paper road surface.

Results of a *patterned* tyre on the mastic asphalt road surface is seen in Figure 3.7. The measurement data set, Figure 3.7a, has an even more distinct peak at 1000 Hz than seen in the spectrum for the slick tyre, Figure 3.2a. The general tendency in the influence of the noise source types is that air-flow related sources become dominant for high frequencies and high speeds, Figure 3.7b. Compared with the results for a slick tyre on the same surface, Figure 3.2b, tyre vibrations have a greater influence also at high frequencies and low speeds. Otherwise the results are very similar with a complete dominance of air-flow related sources at the 400 and 1250 Hz bands. This indicates the relevance of the assumption that the A-coefficients are relatively speed independent.

(a) CPB level as a function of speed and frequency.

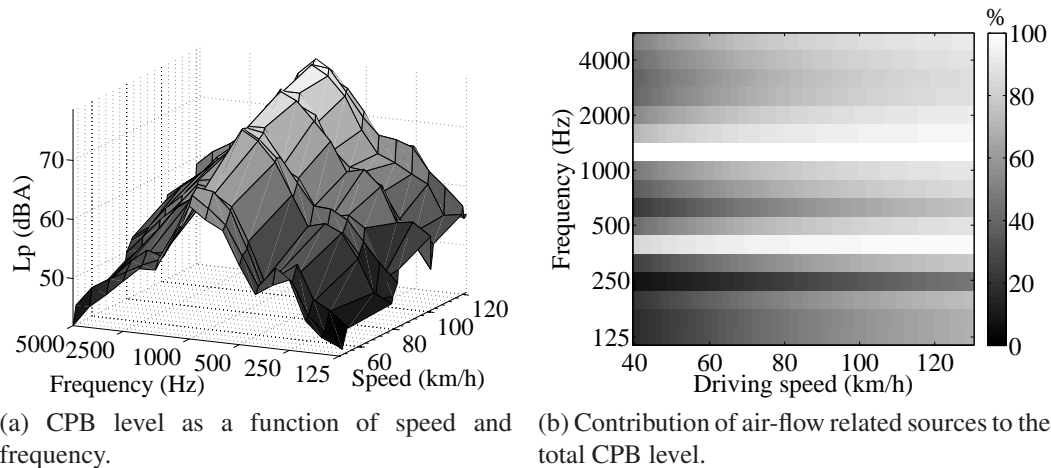(b) Contribution of air-flow related sources to the total CPB level.

Figure 3.7: Results for a *patterned* tyre on a mastic asphalt road surface (compare with the results from a slick tyre, Figure 3.2).

3.4 Calculations

3.4.1 Chalmers tyre/road noise model

The present tyre/road interaction model at Chalmers, presented in e.g. [7, 6, 8] is used to simulate tyre/road noise. The model consists of three main parts:

- A waveguide finite element tyre model.

- A time domain contact model.

- A BEM radiation model calculating the sound due to tyre vibrations.

The waveguide finite element model provides time domain Green's functions for the response of the tyre. These are used in the contact model together with the geometry of the road surface and linear springs accounting for the small scale road roughness. A convolution between the obtained contact forces and the tyre Green's functions gives tyre displacements in present and future time steps due to the present contact forces. The contact calculation start with a loading phase where the tyre is slowly lowered into the road until the right total contact force is reached. Then the tyre starts rolling and a steady state is usually reached after some revolutions. The time signal of the wave field on the tyre, usually from two revolutions, is then converted to the frequency domain. This wavenumber spectrum is input to the boundary element module where the tyre is placed above an infinite plane. The sound pressure level is evaluated on a half sphere around the tyre for each frequency separately. In the tyre/road interaction model, the upper limit of the frequency range is proportional to the driving speed, very high frequency noise can not be calculated for low speeds. The radiation module is the most time consuming part with calculation times in the order of hours or days depending on the computer and the calculation set-up. This limits the number of cases that so far have been analysed with the speed exponent approach.

The results presented in the following section are average sound pressure levels calculated at a half sphere around a slick tyre rolling on the road. The radius of the evaluation surface is one meter with its center in the contact. The wave field on the tyre that is used as input to the radiation model is evaluated after 4 revolutions of rolling on the road surface. Speeds between 40 and 100 km/h are utilised to create data sets similar as for the measurements. Results are shown up to the third octave band of 1600 Hz due to the frequency limitation for low speeds. The roughness of the road is based on multi-track laser measurement of a real surface. Two surfaces are investigated, a smooth ISO surface and a rough asphalt surface with surface dressing 5/8.

3.4.2 Results

The calculated data set for a slick tyre on a smooth ISO surface is seen in Figure 3.8a. It looks similar to the previous measured data with a sharp peak in the spectrum around 1000 Hz. The speed dependency of different frequency bands is easier seen in Figure 3.8b where the percentage of air-flow related sources to the total level in shown. Even in this modelled case, air-flow related sources are important for the generated tyre/road noise at low frequencies, at 400 Hz band and at high frequencies. This is astonishing as the used model does not include any special air-flow related source terms, it only considers tyre vibrations above a rigid road plane. The monopole characteristics found in in the calculated noise must be due to the tyre vibrations. An idea could be that tyre vibrations in/or close to the contact patch "squeezes" air out. In other words that the geometry of the road and the tyre together with tyre vibrations causes acceleration of air and the generation of noise with a speed dependency around U^4.

(a) Calculated sound pressure level as a function of speed and frequency.

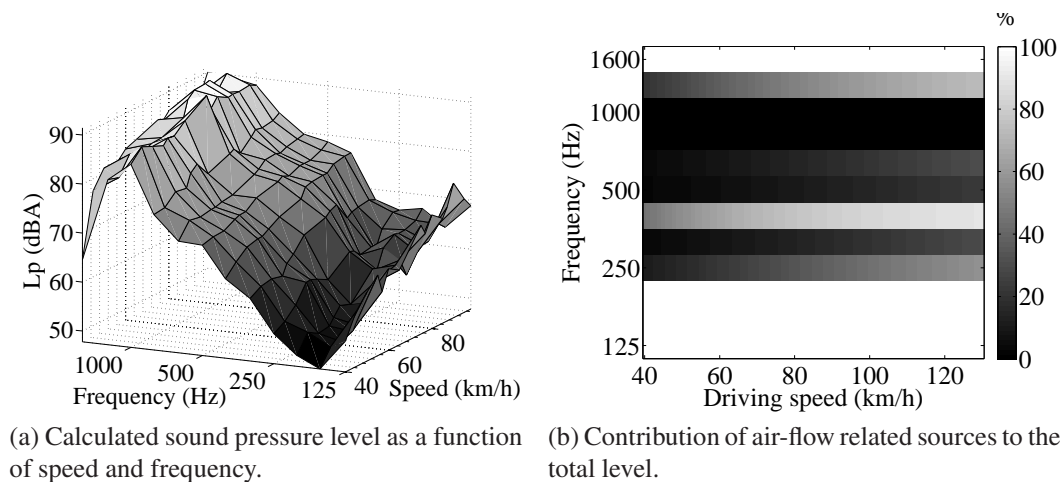(b) Contribution of air-flow related sources to the total level.

Figure 3.8: Calculated results for a slick tyre on an ISO surface.

Studying the results for the ISO surface more in detail, Figure 3.9, some interesting features can be seen. Compared with the measured data there is a relatively small spread in the low frequency data points, Figure 3.9a shows the result for the 160 Hz band. This can be due to fewer noise sources included in the calculations compared with real measurements. Turbulence/wind noise could be one for example. Going a little higher in frequency the spread is even smaller and again the 400 Hz band is dominated by air-flow related sources, Figure 3.9b. And at 800 Hz it is the opposite, tyre vibrations are the only relevant noise source and the fitted curve matches the data well. The spread in the high frequency data is larger than what was commonly found in the measurement data, Figure 3.9d shows the result for the 1250 Hz band.

(a) 160 Hz, concentrated data and nice fit to the U^4 curve.

(b) 400 Hz, clearly dominated by air-flow related sources.

(c) 800 Hz, representing a region dominated by tyre vibrations.

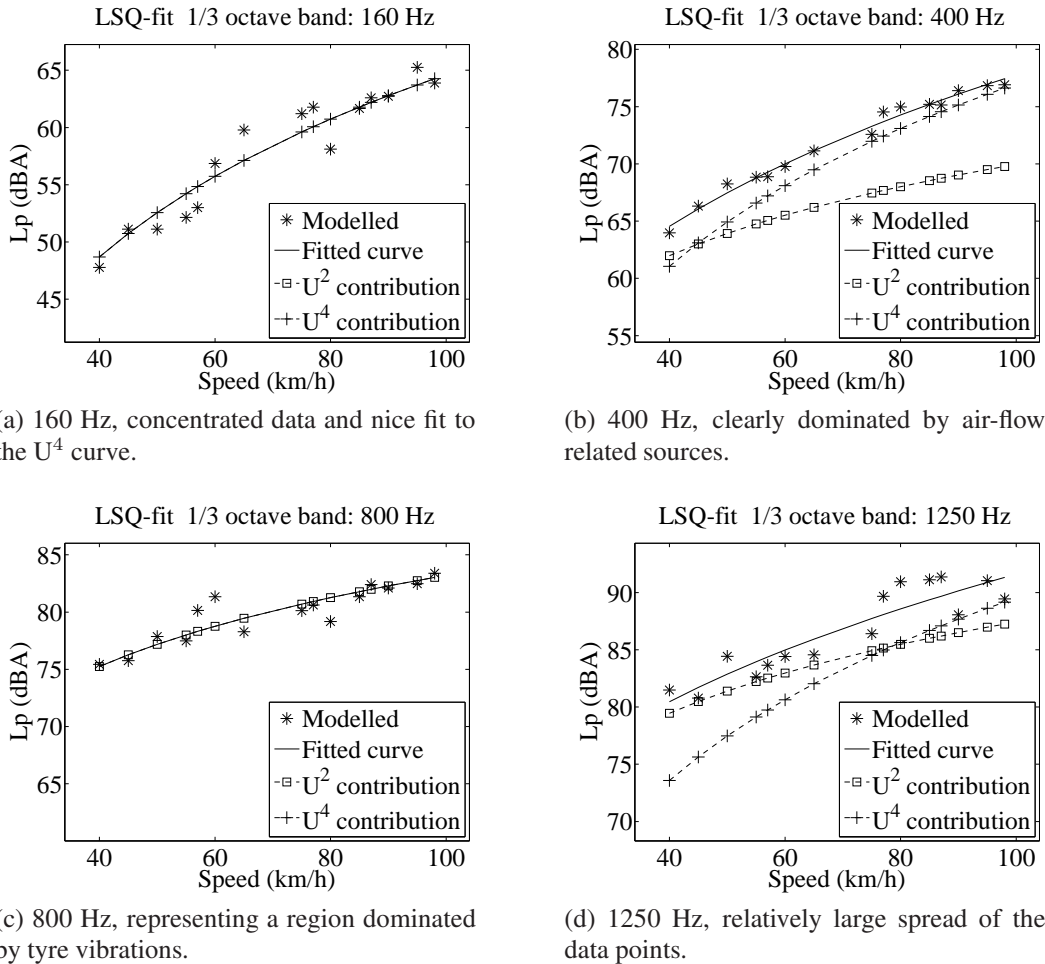(d) 1250 Hz, relatively large spread of the data points.

Figure 3.9: Calculated single third octave band results. Data points and the fitted curve consisting of the contribution from tyre vibrations and air-flow related source mechanisms from calculations of a slick tyre on an ISO surface.

The calculated data set for a slick tyre on a rough asphalt road with surface dressing 5/8 is seen in Figure 3.10a. The spectrum is more flat than for the previous ISO surface, the peak level around 800-1000 Hz is not as pronounced. Figure 3.10b shows the influence of air-flow related sources to the total level. The general tendency is that *both* tyre vibrations (mainly lower speeds) and air-flow related sources (higher speeds) are important for the sound pressure level. Three frequency bands are dominated by air-flow related sources; 160, 400 and 800 Hz.
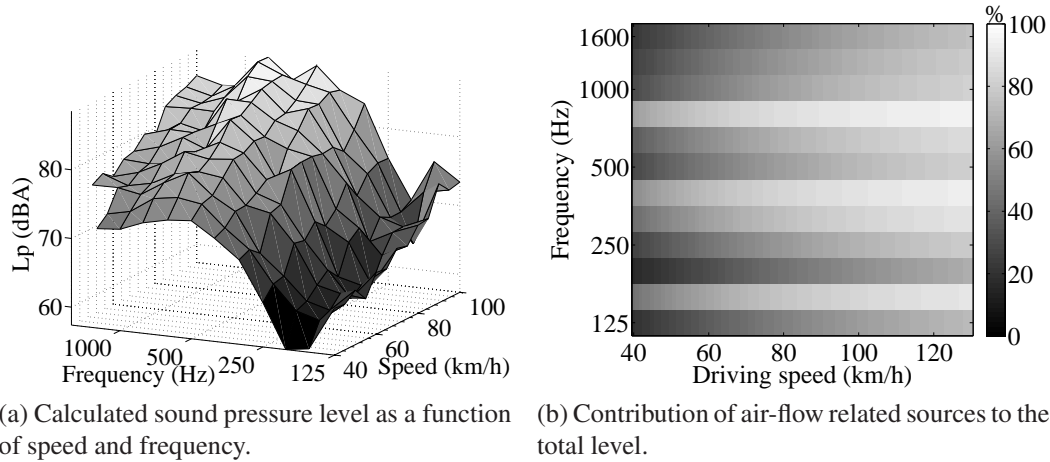
(a) Calculated sound pressure level as a function of speed and frequency.

(b) Contribution of air-flow related sources to the total level.

Figure 3.10: Calculated results for a slick tyre on an rough road with surface dressing 5/8.

Figure 3.11 show two single frequency band results from calculations of a slick tyre on rough road with surface dressing 5/8. Figure 3.11a shows the result for the 160 Hz band where the spread of the data is larger for higher speeds That both types of noise sources are important also for the higher frequencies can be seen in the results for the 1250 Hz band, Figure 3.11b.

(a) 160 Hz, strong speed dependency.
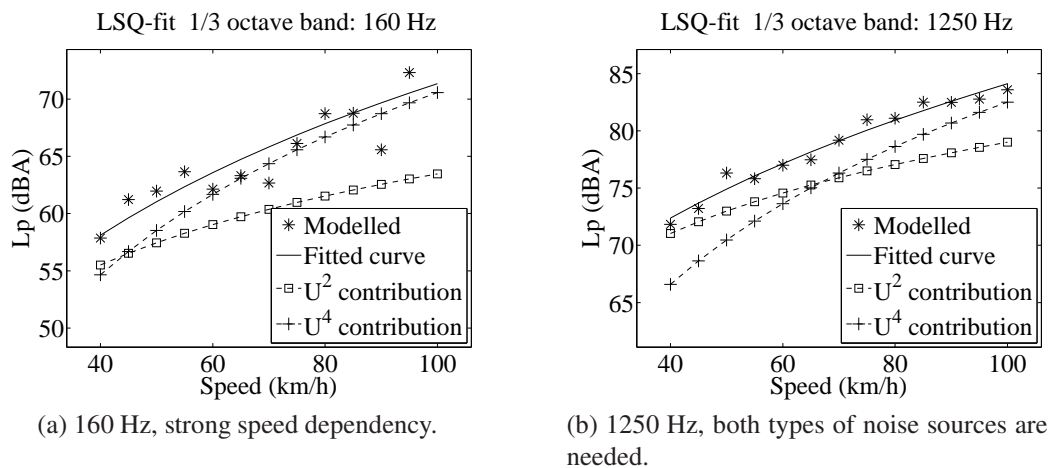

(b) 1250 Hz, both types of noise sources are needed.

Figure 3.11: Calculated single third octave band results. Data points and the fitted curve consisting of the contribution from tyre vibrations and air-flow related source mechanisms from calculations of a slick tyre on an rough road surface.

3.5   Conclusions and future work

The difference in speed dependency of tyre vibrations and air-flow related mechanisms is used to investigate their relative influence on tyre/road noise. The results show a very strong importance of air-flow related mechanisms at high frequencies but surprisingly also at very low frequencies. Especially the 400 Hz band stands out as consequently being dominated by air-flow related sources. Even in the case of a profiled tyre there is a major influence of air-flow related sources.

Tyre/road noise was also calculated with the tyre/road interaction model used at Applied Acoustics, Chalmers University of Technology. The simulation results show contributions of air-flow related mechanisms over the whole frequency range. This is remarkable as the model does not include any individual approach to capture air-flow related mechanisms.

The air-flow related mechanisms that are observed both in measurement and calculations have to be induced by the interaction between the vibrating tyre and the road surface, forcing air to move rapidly in the contact area and creating acoustic source terms with monopole characteristics. When the tyre is moving with similar phase over the cross section, air will be accelerated with minimal hydrodynamic short-circuiting leading to efficient noise radiation. This could also explain the strong air-flow related contribution around 400 Hz where tyre radiation have been found to be mainly determined by the so-called breathing mode of the tyre [8].

The speed exponent approach is based on the assumption that noise from tyre vibrations and air-flow related sources are uncorrelated. If both sources have their origin in tyre vibrations it might cause an uncertainty in the validity of the results. The assumption may however still be valid as the two sources are very different in their character and might have different locations. Further, how correlated the sources are is less important when either of the them dominate the generated noise.

An extension of the analysis on calculated tyre/road noise would be valuable from many aspects. Partly this could be done by investigating the available calculation results further. One could for example look into the directivity of the air-flow related source contribution. This could confirm that the U^4-contribution really origins from the contact patch, at least more than the U^2-contribution.

It would also be of interest to investigate if the the non-linearities of the air-pumping sources suggested in e.g. [19, 27] would have a noticeable effect on the observed speed exponent.

Chapter 4
Conclusions and future work

The first part of this thesis investigates the importance of tread inertia and damping for detailed tyre/road contact modelling. In the second part is the difference in vehicle speed dependency of noise from tyre vibrations and air-flow related mechanisms used to analyse their relative contributions to the total tyre/road noise.

Results from the first part show that the contact simulations are affected when using a simplified tread response that does not include the dynamic character of the material. The significant difference in steady state contact stiffness has been found to depend on the material damping. The effect of tread mass is limited. It is suggested to approximately include the effects of damping as an increased stiffness in a quasi static tread model for moderately detailed tyre/road contact simulations.

Results from the second part show that air-flow related source mechanisms are major contributors to the overall tyre/road noise. Their importance is seen, not only at frequencies above 1000 Hz which is commonly suggested in the literature, but also at very low frequencies and especially at around 400 Hz. The analysis indicates that tyre vibrations in the contact may lead to air-flow related noise with monopole characteristics.

The tread material that is used in the contact simulations has a loss factor that grows with frequency. An extension to the work presented in the first part of this thesis could be to simulate a material which has a different frequency dependence of the loss factor. This could give indications on how general the results and conclusions are. It would also be interesting to evaluate the effect of introducing a speed dependency to the stiffness of linear contact springs in a complete tyre/road interaction model.

There are many things to investigate further in the field of air-flow related source. Analysing measured and calculated noise from a larger number of tyre/road noise combinations could give further insight into what governs this type of generation mechanisms.

Bibliography

[1] WHO, world Health Organisation, Europe - Noise. `http://www.euro.who.int/en/what-we-do/health-topics/environment-and-health/noise`. Visited 2013-05-14 at 11:15.

[2] J. Winroth and P. B. U. Andersson. Implementation of non-linear contact stiffness and adhesion in a numerical model for tyre/road contact. In *Proceedings of InterNoise 2010*, Lisbon, Portugal, June 13-16 2010.

[3] W. Kropp. Structure-borne sound on a smooth tyre. *Applied Acoustics*, 26(3):181–192, 1989.

[4] P. B. U. Andersson, K. Larsson, F. Wullens, and W. Kropp. High frequency dynamic behaviour of smooth and patterned passenger car tyres. *Acta Acustica united with Acustica*, 90:445–456, 2004.

[5] K. Larsson and W. Kropp. A high-frequency three-dimensional tyre model based on two coupled elastic layers. *Journal of Sound and Vibration*, 253(4):889–908, 2002.

[6] C. Hoever. *The influence of modelling parameters on the simulation of car tyre rolling losses and rolling noise*. `http://publications.lib.chalmers.se/records/fulltext/166543/166543.pdf`. Licentiate thesis. Division of Applied Acoustics, Chalmers University of Technology, Göteborg, Sweden, 2012.

[7] C. Hoever and W. Kropp. The influence of modelling parameters on the simulation of car tyre rolling noise and rolling resistance. In *Proceedings of AIA-DAGA 2013*, Merano, Italy, 2013. In press.

[8] W. Kropp, P. Sabiniarz, H. Brick, and T. Beckenbauer. On the sound radiation of a rolling tyre. *Journal of Sound and Vibration*, 331:1789–1805, 2012.

[9] W. Kropp. *Ein Modell zur Beschreibung des Rollgeräusches eines unprofilierten Gürtelreifens auf rauher Strassenoberfläche, (A model for the description of the rolling noise from a smooth tyre on a rough road).* PhD thesis, Fortschritt-Berichte Reihe 11, Nr 166, VDI Verlag, Düsseldorf, 1992.

[10] D. J. O'Boy and A. P. Dowling. Tyre/road interaction noise-numerical noise prediction of a patterned tyre on a rough road surface. *Journal of Sound and Vibration*, 323(1-2):270–291, 2009.

[11] I. Lopez Arteaga. Influence of material damping on the prediction of road texture and tread pattern related rolling resistance. In *Proceedings of ISMA2010 including USD2010*, pages 4039–4052, 2010.

[12] P. B. U. Andersson and W. Kropp. Time domain contact model for tyre/road interaction including nonlinear contact stiffness due to small-scale roughness. *Journal of Sound and Vibration*, 318:296–312, 2008.

[13] J. J. Kalker. *Three-Dimensional Elastic Bodies in Rolling Contact*. Solid Mechanics and Its Applications. Springer, 1990.

[14] F. Wullens and W. Kropp. A three-dimensional contact model for tyre/road interaction in rolling conditions. *Acta Acustica united with Acustica*, 90(4):702–711, 2004.

[15] G. Dubois, J. Cesbron, H. P. Yin, F. Anfosso-Lédée, and D. Duhamel. Statistical estimation of low frequency tyre/road noise from numerical contact forces. *Applied Acoustics*, 74(9):1085–1093, 2013.

[16] F. Liu, M. P. F. Sutcliffe, and W. R. Graham. Prediction of tread block forces for a free-rolling tyre in contact with a rough road. *Wear*, 282-283:1–11, May 2012.

[17] G. Dubois, J. Cesbron, H. P. Yin, and F. Anfosso-Ledee. Macro-scale approach for rough frictionless multi-indentation on a viscoelastic half-space. *Wear*, 272(1):69–78, 2011.

[18] F. Wullens. *Excitation of Tyre Vibrations due to Tyre/Road Interaction*. PhD thesis, Division of Applied Acoustics, Chalmers University of Technology, Göteborg, Sweden, 2004.

[19] M. J. Gagen. Novel acoustic sources from squeezed cavities in car tires. *The Journal of the Acoustical Society of America*, 106(2), 1999.

[20] K. Larsson, S. Barrelet, and W. Kropp. The modelling of the dynamic behaviour of tyre tread blocks. *Applied Acoustics*, 63(6):659–677, 2002.

[21] P. B. U. Andersson. *Modelling Interfacial Details in Tyre/Road Contact - Adhesion Forces and Non-Linear Contact Stiffness*. PhD thesis, Division of Applied Acoustics, Chalmers University of Technology, Göteborg, Sweden, 2005.

[22] International Organization for Standardization. *ISO 10844, Acoustics - Specification of Test Tracks for the Purpose of Measuring Noise Emitted by Road Vehicles*, 1994.

[23] P. B. U. Andersson. *High frequency tyre vibrations*. Licentiate thesis. Division of Applied Acoustics, Chalmers University of Technology, Göteborg, Sweden, 2002.

[24] R. Hayden. Roadside noise from the interaction of a rolling tire with the road surface. In *Purdue Noise Control Conference, Purdue University, West Lafayette*, pages 62–67, 1971.

[25] D. Ronneberger. Towards quantitative prediction of tyre/road noise. In *Proceedings of the Workshop on rolling noise generation, Berlin*, pages 218–235, 1989.

[26] J.-F. Hamet, C. Deffayet, and M.-A. Pallas. Air pumping phenomena in road cavities. In *Proceedings of the International Tire/Road Noise Conference, Gothenburg, Sweden*, pages 19–29, 1990.

[27] S. Kim, W. Jeong, Y. Park, and S. Lee. Prediction method for tire air-pumping noise using a hybrid technique. *The Journal of the Acoustical Society of America*, 119(6):3799–3812, 2006.

[28] F. Conte and P. Jean. CFD modelling of air compression and release in road cavities during tyre road interaction. In *Proceedings of Euronoise, Tampere, Finland*, 2006.

[29] U. Sandberg and J. Ejsmont. *Tyre/road noise reference book*. Informex, Kisa, Sweden, 2002.

[30] T. Beckenbauer et al. Effect of pavement texture on tyre/pavement noise. Technical Report Scientific report no. 847, German Federal Ministry of Transport, Buildings and Dwellings, Bonn, Germany, 2002.